Corresponding Author Pre-print Copy for Self-Archiving

Ocean Modelling, http://dx.doi.org/10.1016/j.ocemod.2014.01.004

Available online 25 January 2014

Simulating surface oil transport during the Deepwater Horizon oil spill: Experiments with the BioCast system

Jason Keith Jolliff[1*] Travis A. Smith[1] Sherwin Ladner[1] Robert A. Arnone[2]

1 - Naval Research Laboratory, Oceanography Division, Stennis Space Center, Mississippi

2 – University of Southern Mississippi, Department of Marine Science

*Corresponding Author: tel:+12286885308 / Fax: +12286884149; email: jolliff@nrlssc.navy.mil

The U. S. Naval Research Laboratory (NRL) is developing nowcast/forecast software systems designed to combine satellite ocean color data streams with physical circulation models in order to produce prognostic fields of ocean surface materials. The Deepwater Horizon oil spill in the Gulf of Mexico provided a test case for the Bio-Optical Forecasting (BioCast) system to rapidly combine the latest satellite imagery of the oil slick distribution with surface circulation fields in order to produce oil slick transport scenarios and forecasts. In one such sequence of experiments, MODIS satellite true color images were combined with high-resolution ocean circulation forecasts from the Coupled Ocean-Atmosphere Mesoscale Prediction System (COAMPS®) to produce 96-h oil transport simulations. These oil forecasts predicted a major oil slick landfall at Grand Isle, Louisiana, USA that was subsequently observed. A key driver of the landfall scenario was the development of a coastal buoyancy current associated with Mississippi River Delta freshwater outflow. In another series of experiments, longer-term regional circulation model results were combined with oil slick source/sink scenarios to simulate the observed containment of surface oil within the Gulf of Mexico. Both sets of experiments underscore the importance of identifying and simulating potential hydrodynamic conduits of surface oil transport. The addition of explicit sources and sinks of surface oil concentrations provides a framework for increasingly complex oil spill modeling efforts that extend beyond horizontal trajectory analysis.

Key words: oil spill model; Gulf of Mexico; ocean circulation; pollutant simulation

Highlights:

- A Eulerian approach to oil spill forecasting is applied to the DWH oil spill.
- Timing of oil landfall simulations was depended on a buoyancy-driven current.
- Longer simulations with oil decay terms demonstrate oil containment in the Gulf.

1. Introduction

On 20 April 2010 the deep-sea drilling unit Deepwater Horizon (DWH) exploded leading to an unprecedented discharge of oil and gas from the Macondo prospect (~77 km southeast of the Mississippi River Delta; Fig. 1) into the Gulf of Mexico for the following 86 days. Estimates for the total amount of oil released during that period range from approximately 4.8-8.3 x 10^8 L (Crone and Tolstoy, 2010, Leifer, 2010). This constitutes the largest accidental marine oil spill in U.S. waters (Levy and Gopalakrishnan, 2010). The total economic impact of the DWH oil spill is estimated to be greater than US $8.7 billion (Sumaila et al., 2012).

The unprecedented scope of the oil spill became obvious as satellite images of the surface oil emerged in the weeks immediately following the DWH blowout. For example, NASA's Moderate Resolution Imaging Spectroradiometer (MODIS) sensors aboard the sun-synchronous Terra and Aqua satellites provided true color images that revealed an apparent oil slick distribution contaminating > 20,000 km^2 of ocean surface over the course of the oil spill event (Hu et al., 2011). Detection of the oil slick extent from passive visible remote sensing is based on the oil slick's modification of sun glint reflectance (Hu et al., 2009). Such detection methods do not provide a direct quantitative assessment of oil concentration or surface oil slick thickness. Nonetheless, the subsequent MODIS and other remote sensing images indicated the oil spill was unfolding as a mesoscale phenomenon (on the spatial order of ~10–1000 km, and temporal duration of weeks to months).

Of paramount concern to government agencies, resource managers, and emergency responders during the DWH oil spill time period (20 April–15 July 2010) and thereafter was the ultimate fate and potential landfall of the extensive offshore aggregation of surface oil. Anticipation of landfall required mobilization of extensive resources to deploy, for example, prophylactic oil boom-type barriers, and to stage secondary defense supply stations in support of cleanup efforts (State of Louisiana, 2010).

The National Oceanic and Atmospheric Administration (NOAA) was the lead U.S. Government agency for oil slick trajectory forecasting. NOAA provided nowcasts of the oil slick distribution by combining aircraft overflights, satellite information, and in situ observations (NOAA OR&R, 2013a). Forecasts of the oil slick distribution (24, 48, and 72 h) were provided from 22 April to 23 August 2010 (*ibid.*). The forecasting was accomplished via the General NOAA Oil Modeling Environment (GNOME) oil spill trajectory model (Zelenke et al., 2012). The GNOME system ingests surface current information from data sources and/or numerical ocean circulation models as well as an initial oil contaminant distribution to project the movement of these contaminants. The primary transport calculation is Lagrangian: i.e., surface oil is represented as virtual "particles" that are tracked over the timescale of the simulation using two-dimensional surface displacement calculations. This is the common method used in oil spill modeling (e.g., Sotillo et al., 2008) and similar Lagrangian particle-based forecast methods were simultaneously employed by the research and academic communities during the DWH oil spill (Liu et al. 2011a; Mariano et al., 2011).

Here we present an alternative method to two-dimensional Lagrangian oil trajectory forecasts. The BioCast system resolves a fully three-dimensional Eulerian transport calculation. These calculations do not require presumptions about virtual particles and instead treat oil as an idealized passive tracer. Both types of oil spill modeling approaches must make assumptions about the nature of oil in water that are imperfect: oil may behave as both particle aggregations and dissolved tracers depending on the state of weathering, dissolution, and other specific material properties of the hydrocarbons under consideration (ASCE, 1996; Leifer et al., 2006). In a fundamental sense, the Lagrangian model particle (or element) is simply a point in two-dimensional space and its formal representation of mass is arbitrary. This is in contrast to the Eulerian methods explored herein: the mass of oil in each spatial discretization (grid cell) defines the model's state variable. This allows for explicit calculation of three-dimensional material transport, weathering (transformation) of materials, and potential changes in material buoyancy. Precedent for Eulerian approaches to oil spill modeling may be found in Tulloch et al. (2011) and Maltrud et al. (2010). Note that in these studies the tracer is described as a generic dye, whereas herein we attempt to move forward with an explicit oil concentration model. With this increase in complexity, however, is the associated disadvantage: the modeler's dilemma, i.e., the need to parameterize and mathematically represent processes that may not be not well constrained with observations or experiment.

Cognizant of these and other inherent complexities, we nonetheless seek to address the remaining core problems posed by operational oil transport forecasting as an oil spill response tool. First, the methods required to rapidly combine satellite-based estimates of the oil spill distribution with state-of-the-art ocean circulation models to produce an oil spill distribution forecast are evaluated. Second, we examine how the inherent reactivity of the contaminants may impact the simulated distribution over time and in contrast to a scenario wherein only the physical transport is considered.

In this paper, two Eulerian transport approaches to oil spill simulation are examined via numerical experiment to address these aforementioned problems. In the first approach (Section 3), the oil transport-forecasting problem is examined in terms of a passive tracer transported at the ocean's surface. Emphasis is placed on the initial spatial distribution estimated from satellite data and the evolution of this distribution over the ensuing 96 h. The results are examined with respect to subsequent observation of oil distribution and landfall. In the second approach (Section 4), more complex computations of potential hydrocarbon sources and sinks are considered. These computations are performed in the context of a longer-term simulation (~18 days) of the oil spill to address the timescale of decay rate processes. Accordingly, a regional ocean circulation model is used to provide coastal surface current information as well as simulate the interaction of the oil slick with the mesoscale circulation in the open Gulf of Mexico.

2. Methods

BioCast is computational software that provides for a rapid combination of ocean circulation model results with a three-dimensional tracer transport-reaction simulation. The flow of information is thus very similar to NOAA's GNOME oil trajectory forecasts: information on surface currents must be combined with some initial state of the material distribution. BioCast was developed for short-term forecasting (~ 24 h) of ocean surface bio-optical properties as detected and estimated by passive remote sensing methods.

However, the software may be applied to any material distribution (such as oil) if the initial state is provided.

The BioCast transport calculation maps the velocity information to a three-dimensional stencil and makes minor adjustments to constrain the velocity field to continuity:

$$-\frac{\partial w}{\partial z} = \frac{\partial u}{\partial x} + \frac{\partial v}{\partial y} \qquad (1)$$

where *w* is the vertical velocity and *u*, *v* are the horizontal velocities in a Cartesian coordinate frame. Following these adjustments, transport is calculated using first-order upstream differences for the advection equation (e.g., Smolarkiewicz, 1984) on the three-dimensional grid. First-order numerical advection schemes are inherently diffusive (*ibid.*). An analysis of the numerical diffusion inherent to our scheme yields horizontal diffusivity values in the range of ~ 50–700 $m^2 s^{-1}$. Studies of natural horizontal diffusion tend to scale with the length scale of the observations (Obuko, 1971). For the length scales commensurate with the distribution of oil slicks within our model domains (~ 50-500 km), estimates of horizontal diffusion are in a similar range (~ 50-1000 $m^2 s^{-1}$; Obuko, 1971; Ledwell et al., 1998).

Thus the BioCast transport calculation represents the advection-diffusion portion of the advection-diffusion-reaction problem. The reaction portion may be modified in the BioCast software or eliminated entirely based on the requirements of the problem and the designs of the investigator. The reaction calculations can range from simple decay rate constants to complex biogeochemical models. Here the reaction portion was modified to describe positive buoyancy, and then subsequently modified to provide an oil source term and to simulate oil weathering, as explained in Section 4.

In both series of experiments, the initial state was based on the MODIS true color imaging of the oil slick distribution on 11 May 2010 (Fig. 2a). As mentioned above, the apparent ocean surface discoloration is based largely on changes in sun glint reflectance due to the oil slick's presence; the varying angular dependence of sun glint makes quantitative retrieval of oil slick thickness or quantity from these images very difficult (Hu et al., 2009). Accordingly, the image was decomposed to develop a novel algorithm for determining the spatial extent of the oil slick. Image pixels where oil is presumed to be present (based strictly on the apparent contrast with the surrounding open ocean image pixels) are analyzed for the scaled red (R) and green (G) image values (ranging from 1-255). This is repeated (~10 times) to develop an approximate range of values for apparent oil-influenced surface water discoloration in the true color image. Once a set of thresholds is established, all of the oil-containing pixels are identified via automated image processing software. This procedure must be repeated and adjusted for any new RGB image because the RGB true color data processing will render different scaled RGB values based on the amount of sun glint reflectance present in the raw satellite data. A similar procedure was also used to remove the presence of clouds, again based on the RGB values where clouds were presumed to be present. Image pixels identified as oil (Fig. 2b) were then mapped to the corresponding latitude and longitude coordinates of the model domain, and thereby provided a starting place for forward integration of the transport computations (Fig. 3). Additional steps to initialize the surface oil concentration on a more quantitative basis are explained in Section 4.

There is uncertainty in this initial surface oil distribution. Other concurrent satellite analyses depict additional surface oil west and north of our estimate (Hu, 2010), and potentially smaller oil slicks detached from the main bolus near the DWH site (NOAA/NESDIS, 2013). We note that synthetic aperture radar (SAR) sensors also provided satellite-based estimates of surface oil slick locations during the event that may have been substantially different from MODIS sun glint-based analyses (Walker et al., 2012). Future work will aim towards a more comprehensive assimilation of satellite information with associated uncertainty estimates into oil spill models.

An initial set of numerical experiments was performed using the Coupled Ocean-Atmosphere Mesoscale Prediction System (COAMPS®), a nested modeling system developed at the Naval Research Laboratory that allows for a two-way exchange of information between the atmospheric and oceanic forecasting components. The nonhydrostatic atmospheric COAMPS model component (Hodur, 1997) is the operational mesoscale forecasting system for the U.S. Navy. The hydrostatic Navy Coastal Ocean Model (NCOM; Martin, 2000; Barron et al., 2004; Kara et al., 2006) served as the oceanic component. NCOM is the main regional oceanographic forecasting model for the U.S. Naval Oceanographic Office (Rhodes et al., 2002).

The atmospheric and oceanic model coupling was designated via the upper-most oceanic model grid cell temperature and the lowest grid cell atmospheric model variables (temperature, humidity, wind velocity, pressure, and radiative fluxes). At a 6-min coupling interval, bulk fluxes of heat energy exchange were calculated following the Coupled Ocean-Atmosphere Response, version 3 (COARE 3.0) scheme (Fairall et al., 1996). Further details of the COAMPS modeling components are listed in Small et al. (2012). Verification and validation of the COAMPS forecasting system may be found elsewhere (Doyle et al., 2009; Small et al., 2012); here we focus on how the forecasts of surface currents from COAMPS may be used by the BioCast system to forecast surface oil transport. Only the "true" hourly surface current forecast fields forward from the analysis time (the initial state on 11 May 2010) were used. This means that the surface current velocities were genuine forecasts of marine conditions from the modeling system; i.e., no data assimilation of atmospheric or oceanic data beyond the analysis time occurred.

The estimated surface oil distribution from the 11 May 2010 MODIS image was used to initialize a relative oil concentration state variable. The oil concentration was treated as a passive tracer (physical transport/no biological-chemical reactions) with no additional sources beyond the initialization field. Hence the conservation equation may be simply expressed as:

$$\frac{\partial RC}{\partial t} = -\left(\frac{\partial u}{\partial x} + \frac{\partial v}{\partial y} + \frac{\partial w}{\partial z}\right) RC + \mathfrak{B}\left(\frac{\partial C}{\partial z}\right) \qquad (2)$$

The state variable, RC, is a relative concentration of oil. This value was initialized as 100 where the MODIS true color threshold-based algorithm suggested the presence of oil.

The transport calculation treats the surface oil as a dissolved tracer. This permits downwelling (downward vertical advection) as well as diffusion into grid cells beneath the surface. Whereas this may indeed be the fate of some dissolving or emulsified hyrdocrabons, a positive buoyancy term ($\mathfrak{B}$) was nonetheless added to the calculation (Eq. (2)) to force the simulated hydrocarbons back into the surface grid cell. This calculation does not permit downward vertical penetration of simulated oil but it will still allow for surface convergence or divergence (dispersion) of materials.

Once again, this is in contrast to Langrangian methods. Physical dispersion cannot be explicitly defined for a single point in space subject to a horizontal displacement calculation. Statistical methods must be employed to apply a probabilistic modification of the trajectory; e.g., the random walk method (Proehl et al., 2005). Veracity of these statistical methods generally improves with an increase in the number of representative Lagrangian particles or alternatively, an ensemble of trajectory model simulations (Brickman and Smith, 2002). As the number of trajectory particles tracked (or ensembles) increases, however, so does the computational expense. Finally, one arrives near the impractical end of that continuum and may elect to instead perform a Eulerian computation that explicitly calculates the mass flux of distributed materials in a single iteration. The disadvantage now is that the representation of the oil's mass as uniformly distributed over the discrete spatial resolution of the model may tend to result in overly dispersive transport. Here, the vertical dispersion is eliminated via a buoyancy restoring term. Horizontal dispersion remains. A consequent criticism of this Eulerian framework specific to oil spill modeling is that "it is practically impossible to detect exactly the oil spill boundaries in a specific moment" (Lonin, 1999). This is in contrast to a spatial distribution of Lagrangian elements that provides a very discrete oil spill boundary. As a practical matter, however, this criticism is easily addressed. One approach is to scale the Eulerian tracer field to the initial source concentration (as in Maltrud et al., 2010; and here, Section 3). Another approach is to define the horizontal oil spill boundary using a lower limit of detection, or threshold value (as in Section 4).

3. COAMPS-based forecast results

The 24-h forecast shows the lateral spreading of the initial relative concentration (RC) field. The northwest corner of the oil slick is initiating contact with the Mississippi River Delta (MRD; Fig. 4a). The 48-h forecast indicates this oil is being transported clockwise around the Southwest Pass of the MRD and initiating landfall on the southern coast of Plaquemines Parish, Louisiana and towards Barataria Bay (Fig. 4b). Some ~74 h forward into the forecast period, this clockwise conduit around the MRD funnels increasing amounts of the initial surface oil distribution into the Louisiana Bight to make significant landfall along the outer islands of Barataria Bay, including Grand Isle and southwest towards Port Fourchon (Fig. 5a). At the conclusion of the forecast period (96 h; the full sequence is provided in Animation 1), this pattern persists and much of the remaining oil from the initial distribution is being transported westward into an apparent onshore/offshore bifurcation in the surface oil distribution (Fig. 5b). Smaller amounts of oil have also been transported northwest towards the Chandeleur Islands and into Breton Sound. Comparatively, however, a far larger amount of the initial oil is transported into the Louisiana Bight to ultimately make landfall at coastal Louisiana locations west of the MRD.

The oil transport patterns are explained by the concurrent surface current forecasts obtained from COAMPS (Fig. 6a). Large velocity surface currents (~ 1.3 m s^{-1}) are moving clockwise around the MRD. This circulation feature is coherent and well-established by approximately 48 h and persists through the remainder of the forecast period (Fig. 6b). There is also a bifurcation in the surface flow ~45 km south of the MRD that explains the apparent offshore/onshore divergence in the simulated surface oil patterns (Fig. 6a and b).

This forecast of oil transport was qualitatively accurate. Oil from the DWH spill was observed making landfall in the vicinity of Port Fourchon on 14 May 2010 (Schmidt, 2010). Ground observations reported by the Shoreline Cleanup Assessment Technique (SCAT) teams indicate initial landfall of oil on 14 May 2010 along the Louisiana coast from Port Fourchon to Grand Isle (NOAA OR&R, 2013b). Heavier amounts of surface oil were sighted in the vicinity of Grand Isle, Louisiana on 20 May 2010 (Rioux, 2010). By 23 May 2010, SCAT data indicate heavy landfall of oil occurring from Port Fourchon to Barataria Bay. This was followed by some of the most significant landfall of surface oil associated with the DWH event (OSAT-2, 2011). The salt marshes of Barataria Bay were also some of the most severely oiled coastal habitats (Michel et al., 2013; Zengel and Michel, 2013).

In addition to the ground observations, the forecast results are confirmed by concurrent analysis of satellite imagery. NOAA National Environmental Satellite, Data and Information Service (NESDIS) satellite composite analysis, which incorporates MODIS data, SAR data, and other sensors (NOAA/NESDIS, 2013), verifies the movement of large oil slicks into the Louisiana Bight on 17 May 2010 (Fig. 7a and b). The 20 May 2010 analysis suggests the conduit around the Southwest Pass was indeed persistent. Additional oil more than 45 km directly south of the MRD would also support the bifurcation in surface currents depicted in the COAMPS forecast and manifest in the simulated oil distributions. The 23 May 2010 NOAA/NESDIS analysis indicates surface oil in Breton Sound and around the Chandeleur Islands (Fig. 7c). SCAT data confirm concurrent landfall in Chandeleur Sound. The 23 May NOAA/NESDIS analysis also depicts oil entering Barataria and Terrebonne Bays (Fig. 7c).

Given the qualitative agreement between forecast and observations, it is probable that the forecast surface current fields have some fidelity to genuine surface currents between 11 and 19 May 2010. However, our forecasts based on the 11 May 2010 initialization apparently accelerated the landfall of significant surface oil slicks upon Grand Isle, Louisiana and vicinity to 14 May 2010, whereas observations suggest heavy landfall of oil did not truly commence until ~19-20 May and thereafter. The SCAT data record of landfall in these areas on 14 May 2010 is documented as “very light,” i.e., consisting of isolated pockets of tar balls and scattered emulsified oil aggregations. Other ground observations verify this description (Schmidt, 2010). More severe categories of land surface oiling appear to commence in the SCAT record around 20 May 2010. Part of the temporal discrepancy between our forecast and observations may be due to oil weathering and the application of dispersants. These processes were not represented in these COAMPS-based forecasting experiments. Another possibility is that landfall of oil is a process that is distinct from shoreward progression and its simulation requires model parameterizations of winds, surface waves, and littoral tidal processes below the spatial resolution of our models.

Another potential source of the temporal mismatch may be associated with the development and intensification of a buoyancy current along the MRD and the upper Louisiana Bight. Generally, buoyant spreading of low salinity water from a river mouth/delta or estuary in the Northern Hemisphere will propagate with land to the right (looking down current) (Simpson, 1997). Along the Louisiana Bight and Louisiana-Texas coasts, this recurrent coastal circulation feature, augmented by southeasterly winds, is known as the Louisiana Coastal Current (LCC) (Wiseman and Dinnel, 1988).

Mississippi River discharge data (Tarbert Landing, MS) provided by the United States Army Corps of Engineers indicate below historical values from 20 April to 11 May 2010 (Fig. 8). This may partly explain the temporal mismatch between simulated and observed oil slick landfall: the simulated buoyancy current was well established by 13 May whereas the true currents may have been less intense until sustained freshwater discharge out of the MRD was sufficient to accumulate a substantially larger buoyancy plume.

This buoyancy current is a recurrent and characteristic feature in this area (Rouse et al., 2005). It is thus highly probable that any oil spill in the vicinity of the MRD will make landfall along Grand Isle, Louisiana and the adjacent coastal sections of the Louisiana Bight. This landfall would encompass Plaquemines, lower Jefferson, and LaFourche Parishes and would potentially propagate farther west to Terrebonne Bay (see Fig. 1). Emergency managers and government agencies should be cognizant of this probability.

4. Regional source/sink experiments

4.1. Velocity fields and oil initialization

The first series of experiments represented the surface oil as a buoyant tracer and focused on a 96-h forecast within the inner nest (500 m horizontal resolution) of a nested ocean modeling domain. For a second set of numerical experiments, the domain was expanded to include the entire Gulf of Mexico and incorporate results from a regional ocean circulation model. The Intra-Americas Seas Nowcast/Forecast System (IASNFS; Ko et al., 2003) provided regional (~ 3 km horizontal resolution) flow fields for integration into the BioCast system. IASNFS is a regional application of NCOM. The Navy Operational Global Atmospheric Prediction System (NOGAPS) provided atmospheric surface forcing (Rosmond, 1992).

These series of experiments are not true forecasts in the sense that the ocean circulation model results are taken from the analysis fields. The term “analysis fields” refers to the assimilation of satellite data into the modeling system via the Modular Ocean Data Assimilation System (MODAS) (Fox et al., 2002). MODAS assimilates remotely-sensed sea surface temperature (SST) and sea surface height (SSH) data that have been optimally interpolated (Bretherton et al., 1976) onto a two-dimensional grid. Potential subsurface temperature departure from a long-term climatology (U.S. Navy Master Ocean Observation Database – MOODS) is then calculated based on regression coefficients that derive subsurface temperature from SSH and SST. The result is a synthetic three-dimensional temperature field. The combined SST and SSH assimilation provides fidelity to the mesoscale dynamics in the Gulf of Mexico, which is critical to forecasting the regional-scale circulation. MODAS synthetics have been previously used to examine biophysical patterns in the Gulf (Jolliff et al., 2008). The archived IASNFS analysis fields are more properly considered “hindcasts.”

Oil initialization was again based on the MODIS 11 May 2010 image. An accurate quantitative estimate of surface oil concentration based solely on sun glint reflectance in a satellite image is not presently feasible. However, it is reasonable to presume there is some minimum threshold of oil presence at the ocean surface that must be reached before any detection with passive visible remote sensing techniques may occur. Modification of sun glint reflectance by surface oil suggests the presence of oil in sufficient thickness to suppress short surface waves (Adamo et al., 2009). With respect to operational monitoring, an oil “slick” is defined as oil of sufficient thickness to dampen surface waves (NOAA OR&R, 2012). Based on charts adapted from the Bonn Agreement Oil Appearance Codes (BAOAC) (*ibid.*), minimum satellite detected oil slick thickness is estimated to be 2.5 μm. Note that this is different from the minimum thickness visible to the human eye. Here the estimate is focused on the minimum thickness for MODIS sun glint-contaminated images of surface oil. Using a standard reference density for Texas crude oil (873 kg m^{-3}), the model is initialized at 2180 mg oil per m^{-2} of ocean surface for those grid cells where we presume the presence of oil from the MODIS true color image (Fig. 2b).

The initial concentration values are determined by dividing the initial per unit area value (2180 mg oil m^{-2}) by the depth of the surface grid cell. As before, a positive buoyancy restoring term maintains the oil in the model's surface grid cells. The model results are converted back to a per unit surface area basis for analysis (Fig. 9a). In reality, some hydrocarbons may be dissolved whereas much remains at the surface to form slicks and sheen. If one assumes all of the simulated oil per unit area in the model is at the surface in the form of a surface slick, then the thickness of the slick (or sheen) may be calculated using the reference density.

4.2. Source term

Here we consider a source term based on oil apparent at the ocean's surface. Oil entering the water at depth (~1500 m) was not explicitly modeled. There are likely many processes impacting oil injected at depth that curtail its subsequent appearance at the surface (Socolofsky et al., 2011; Joye et al., 2011). For this reason, an initial source term was added at the surface of the DWH site: 32.2 L s^{-1}, or approximately 17,500 barrels per day (BPD). This estimate was based on the surface mass balance estimates provided by the National Incident Command, Flow Rate Technical Group (13,000–22,000 BPD) (McNutt et al., 2011). Once again applying a standard reference density for Texas crude, a mass flux of 28 kg oil s^{-1} is added at the grid cell encompassing the DWH site within the model domain.

4.3. Sink term

A simple first-order decay rate estimate provided a sink term to account for evaporation, weathering and removal processes other than physical transport. Evaporation of crude oil has been shown to follow simple decay rate kinetics (Fingas, 1995), and evaporation is an important process with respect to mass balance of surface oil (National Research Council, 2003). Given that "Mississippi Canyon 252 crude oil" (Belore et al., 2011) will experience 45% loss from surface evaporation after 2 weeks (ibid.), and given a first-order decay rate relation:

$$\ln\left(\frac{C}{C_0}\right) = -rt \qquad (3)$$

the decay rate constant (r) is 4.9 x 10^{-7} s^{-1}. The decay term in the model is then simply:

$$C = C_0 e^{-rt} \quad (4)$$

The processes contributing to the weathering and removal of surface oil are multifaceted and complex. Biodegradation may remove some lower molecular weight hydrocarbons from the bulk crude oil on much shorter timescales, whereas higher molecular weight compounds may be much more recalcitrant to biodegradation and weathering processes (Atlas and Hazen, 2011). The point of this numerical simplification is simply to establish the timescale of the overall oil slick degradation. Obviously, some components of the crude would require (r) values in Eq. (4) much larger or smaller than 4.9 x 10^{-7} s^{-1}; however, incorporating this higher level of complexity into the simulation requires significant expansion of the state variable space, and hence demands for additional detailed knowledge of source concentrations and chemical composition.

Given these considerations, the conservation equation for surface oil is given as

$$\frac{\partial C}{\partial t} = -\left(\frac{\partial u}{\partial x} + \frac{\partial v}{\partial y} + \frac{\partial w}{\partial z}\right) C + \mathfrak{B}\left(\frac{\partial C}{\partial z}\right) + \alpha(i,j) - rC \quad (5)$$

where the change in surface oil (C; mg oil per m^3 ocean surface) with respect to time is the transport calculation plus ($\mathfrak{B}$), the buoyancy calculation, and the source/sink terms. The source term (α) is zero everywhere except the surface location (i, j) of the DWH site, and *r* is the universal decay rate constant.

4.4. Regional source/sink simulation results

Large portions of the DWH oil slicks are simulated to entrain into the outer edge of the Loop Current (Animation 2), as indicated by the IASNFS model's sea surface height contours (Fig. 9a). This large anti-cyclonic feature in the northern Gulf is almost pinching off from the Loop Current to form a warm-core eddy. The large extension of oil slick into the Gulf simulated on 17 May is qualitatively similar to the MODIS true color image captured on 17 May (Fig. 9b and c). It is reasonable to conclude that such oil features (once transported into the Loop Current) will likely transit out of the Gulf and into the Florida Straits. Indeed, there was speculation supported by trajectory model evidence during the oil spill that this may potentially occur (Nelson, 2010). As the oil spill proceeded, however, no significant surface oil transport out of the Gulf of Mexico was observed (Liu et al., 2011b).

The hindcast simulations suggest two main reasons for this failure to egress the Gulf. First, much of the simulated oil initially transported offshore appears to recirculate within a cyclonic eddy associated with the Loop Current. Walker et al. (2012) refer to this feature as a Loop Current frontal eddy and document its evolution during the oil spill. In our simulation, the remaining surface oil does not genuinely entrain into the outer Loop Current until such time as this larger anti-cyclonic circulation feature has finally detached to form a Loop Current Eddy (LCE). A secondary and augmenting mechanism of Gulf containment in our simulation is the decay rate term that significantly degrades simulated surface oil and thereby reduces its horizontal extent.

Regarding the LCE, such anti-cyclonic circulation features frequently detach from the Loop Current and propagate westward in the Gulf (Leben and Born, 1993), and such events are often associated with the appearance of cyclonic circulation features (Biggs et al., 1996). Two cyclonic circulation features are evident on 17 May (Fig. 9a): one where the inchoate LCE appears to be detaching from the Loop Current, and another at the top of the LCE where the leading edge of the simulated oil plume appears to be entering a convergent circulation feature. In the simulation, the surface oil is recirculating within this this feature (Fig. 9a) whereas in the MODIS image the oil “trail” extending into the Gulf appears to be just beginning a turn towards the northeast at its apparent terminus (Fig. 9c). This feature is also depicted in the 17 May NOAA/NESDIS analysis (Fig. 7a).

Some ~2 days forward in the simulation, the offshore oil still appears to be circulating in the cyclonic frontal eddy northeast of the main LCE (Fig. 10a). Corroborating evidence of this surface entrapment of oil within a convergent circulation pattern is shown in the 20 May satellite analysis image (Fig. 7b). This general offshore pattern of surface oil persists into 22 May with the addition of some trace amounts of oil penetrating around the periphery of the LCE, which has now finally detached from the Loop Current (Fig. 10b). Note that the contour intervals in the oil plots terminate at 10 mg oil m^{-2} of ocean surface. Given the assumptions presented in Section 4.1, this would correspond to surface oil sheen of approximately 0.01 μm in thickness. This is below the minimum threshold of surface oil appearance in the BAOAC charts (0.04 μm; NOAA OR&R, 2012). Thus only a trace amount of oil appears to finally transit around the periphery of the LCE.

To elucidate the potential role of degradation/weathering in the simulated oil distribution, a second experiment was performed wherein the decay rate constant (r) was set to zero: a no loss (NL) simulation. All other aspects of the simulation were identical to the initial case. In the final output frame of both simulations, 17.5 days after the initial start-up, the same overall spatial distribution is evident (Fig. 11). As earlier, some offshore oil is recirculating in a cyclonic frontal eddy northeast of the LCE and some trace of oil is beginning to circulate around the outer edge of the LCE. The leading edge of this oil plume extends approximately 360 km farther in the NL simulation (Fig. 11b). Elsewhere, the NL simulation depicts larger amounts of oil at the surface where oil is present.

The role of simulated decay in the surface oil distribution is explored further with a sensitivity analysis of the decay rate constant. The horizontal extent of surface oil in NL simulation (defined by the 10 mg m^{-2} surface oil isopleth) is reduced by 42% when the decay rate constant (*r*) is present and increased by a factor of four (Fig. 12a). Surface oil concentration is also evaluated at three different locations for the final frame of the simulation (17.5 days): (1) 26 km southwest of the DWH site, (2) in the center of the cyclonic frontal eddy (277 km from DWH), and (3) along the outer edge of the LCE (464 km from DWH; Fig. 12). The far field sites (2 and 3) are significantly impacted by the decay rate (Fig. 12b). If (*r*) is increased by a factor of four then the final concentration for both sites is reduced to below 11% of the corresponding NL simulation value. These results reveal a very large sensitivity for the far field sites between 0.25r to 4r (~82% to <

11%). This corresponds to a half-life decay of 65.5 down to 4.1 days. In contrast, the near field site (1) concentrations are all greater than 60% of the NL value over the entire range of (*r*) values.

5. Discussion and conclusions

These regional Gulf of Mexico oil spill simulations demonstrate how the southern Florida coastline was spared contact with any significant bolus of surface oil due to the fortuitous arrangement of mesoscale circulation features and the subsequent detachment of a warm-core eddy from the Loop Current. Had this not occurred, however, our simulations suggest that the weathering and decay of the surface oil may have mitigated any potential impact. We note that this analysis is focused on the movement of the main surface oil aggregations; subsurface plumes of oil may have penetrated to peninsular Florida's west coast (Paul et al., 2013). Our decay rate is based principally on the surface crude oil evaporation rate (Belore et al., 2011) — simulated subsurface oil would require a different parameterization.

The observed transport of oil around the MRD into the Louisiana Bight, and then ultimately shoreward to Grand Isle was well captured by the COAMPS-based oil forecast. Coastal Louisiana's comparative misfortune was due not merely to its proximity to the DWH site, but also due to the sustained surface conduit provided via a buoyancy-driven current along the Southwest Pass. Due to the unique cross-shelf geomorphology of the MRD, there is very little distance between the MRD and the open Gulf of Mexico. Indeed, the shelf-break between the MRD and the Mississippi Canyon may serve as an important area of cross-shelf water mass exchange. Both simulations and observations of the DWH oil trajectories suggest this is the route the oil took to transgress the outer continental shelf (50–200 m isobaths; see Fig. 1) and precipitate a substantial landfall of oil along Louisiana's coastline.

This finding may be critical to understanding future distributions of potential oil spills in the Gulf. In general, currents over the continental shelf (< 200 m depth) have a tendency to flow along isobaths (alongshore) and deep-ocean properties are constrained from transgressing the continental shelf, as predicted by Taylor-Proudman theory (*see*

Brink, 1998, *and also* Weisberg and He, 2003). Identification of specific areas and mechanisms that permit 'open Gulf' to 'shelf' water mass exchanges is required to anticipate the fate of significant oil spills in the major extraction region of the northern Gulf of Mexico. To date, areas in the Gulf where the mesoscale circulation impinges on the shelf and the region around the MRD appear to constitute significant areas of open ocean-to-shelf water mass exchange (Biggs and Muller-Karger, 1994; Weisberg and He, 2003; Jolliff et al., 2008). Note that accurate forecasting would then require regional-scale knowledge of the circulation (Loop Current and associated eddies) as well as local scale knowledge of freshwater discharges in the MRD and potentially other sources.

These simulations did not consider oil as a distinct surface layer capable of responding to wind stress independently of the ocean surface. Other simulation efforts have attempted to consider this behavior explicitly (Sobey and Barker, 1997; Zelenke et al., 2012). Nonetheless, the qualitative agreement between our simulated 17 May 2010 regional oil distribution and the 17 May satellite data (Fig. 7a and Fig. 9b) suggests that this surface layer effect may be less critical when dealing with mesoscale magnitude oil spills in the open ocean. It is not well known how the sea state in the open ocean will modify surface oil slick trajectories given the potential mechanical disruption of the oil slick, particularly at micron-scale thicknesses. There is some evidence that explicit wind-on-oil parameterizations may not be required away from sheltered bays and harbors (Huntley et al., 2011). Other studies seem to suggest explicit wind-on-oil considerations are indeed requisite (Sobey and Barker, 1997; Le Henaff et al., 2012). A more comprehensive modeling treatment would require more detailed knowledge of how oil of varying surface thicknesses and chemical composition will respond to wind forcing, sea state, and the three-dimensional hydrodynamic field.

Wind terms notwithstanding, both the COAMPS-based and regional oil spill simulations presented here support the assertion of Liu et al. (2011a): in the practice of oil spill modeling, ocean circulation is fundamental to all else. A key to both sets of experiments is the simulation of hydrodynamic conduits that may expedite the transport of surface materials from the accident site to areas of particular concern. Additional considerations are then contingent upon the scales of time and space under scrutiny. In the COAMPS experiments, simulated landfall at Grand Isle, Louisiana was accelerated by comparatively swift coastal currents (~1.3 m s^{-1}) contrasted against a background of much more nominal surface current velocities (~ 0.2 m s^{-1}). Over a distance on the order of ~100 km, the timescale of transport for materials captured by this current is ~ 21 hours. On a regional scale, the Loop Current presents a similar velocity hydrodynamic conduit for surface materials (~1.2 m s^{-1}). However, a consideration of Loop Current transport of surface materials from the northern Gulf to the Florida Keys and beyond increases the transport length scale by an order-of-magnitude (~1000 km). The associated transport timescale (~10 days) is now more commensurate with our estimate of the half-life for surface crude oil (~16 days; Equation 4). Thus weathering concerns become much more pertinent to surface oil forecasts with the increase in transport time/space scales.

A remaining uncertainty in this discussion is the usage of dispersants. Over 6 x 10^6 L of dispersants were released during the DWH event (Judson et al., 2010). These materials are designed to break up the hydrocarbons so as to accelerate weathering, biodegradation, and physical dispersion. A key remaining question is whether or not dispersants were applied in sufficient quantities to significantly modify the scaling analysis presented above. We note, however, that by modifying/eliminating the buoyancy restoring term and increasing (r) in Eq. (5), our simulations may be able to provide an upper-limit estimate of dispersant effectiveness and mitigation.

In conclusion, we have presented a proof-of-concept oil spill transport forecasting method based on the BioCast system and input data from operational ocean circulation models and satellite imaging of the ocean. Given that offshore drilling will continue in the northern Gulf of Mexico for the foreseeable future, it is probable that oil spills of some magnitude may occur again. Shorter term (out to 96 h) surface oil spill forecasting – with particular emphasis on potential landfall/beaching of large oil slicks – is critically dependent on accurate ocean current forecasts and knowledge of where cross-shelf water mass exchanges are likely to occur. In our particular example, this cross-shelf exchange is critically dependent on accurate shoreward fluxes of buoyancy. Longer-term simulations for oil slick transport, likely required when oil spills are of regional scale, need to more carefully consider the intrinsic dynamics of oil weathering processes and potential oil source terms. By considering both the timescales of the degradation processes in concert with material transport pathways driven by the ocean circulation, our simulations did not indicate any significant surface oil contamination beyond the northern Gulf of Mexico. Computer simulations used in the future for oil spill response must consider the timescales of all the processes involved.

Acknowledgements: This research was funded by the Naval Research Laboratory 6.2 project "Resolving Bio-Optical Feedback to Ocean/Atmosphere Dynamics." Authors thank D. S. Ko for providing IASNFS ocean circulation model results. Authors thank Stephanie Anderson for help with some of the graphics. Authors also thank Louisiana State University's Earth Scan Laboratory for providing geo-referenced MODIS image files. The authors also thank three anonymous reviewers for comments that improved the manuscript.

Appendix A. Supplementary data

Supplementary data associated with this article can be found, in online version, at http://dx.doi.org/10.1016/j.ocemod.2014.01.004.

References

Adamo, M., G. De Carolis, V. De Pasquale, and G. Paquariello. 2009. Detection and tracking of oil slicks on sun-glittered visible and near infrared satellite imagery. International Journal of Remote Sensing **30**:6403-6427.

ASCE. 1996. State of the art review of modeling transport and fate of oil spills (Task Committee of Modeling Oil Spills of the Water Resources Engineering Division). Journal of Hydraulic Engineering **122**:594-609.

Atlas, R. M. and T. C. Hazen. 2011. Oil Biodegradation and Bioremediation: A Tale of the Two Worst Spills in U.S. History. Environmental Science and Technology **45**:6709-6715.

Barron, C. N., A. B. Kara, H. E. Hurlburt, C. Rowley, and L. F. Smedstad. 2004. Sea surface height predictions from the Global Navy Coastal Ocean Model (NCOM) during 1998-2001. Journal of Atmospheric and Oceanic Technology **21**:1876-1893.

Belore, R., K. Trudel, and J. Morrison. 2011. Weathering, Emulsification, and Chemical Dispersibility of Mississippi Canyon 252 Crude Oil: Field and Laboratory Studies. International Oil Spill Conference Proceedings: March 2011, Vol. 2011, No. 1, pp. abs247, Portland, Oregon.

Biggs, D. C., G. S. Fargion, P. Hamilton, and R. Leben. 1996. Cleavage of a Gulf of Mexico Loop Current eddy by a deep water cyclone. Journal of Geophysical Research **101**:20629-20641.

Biggs, D. C. and F. E. Muller-Karger. 1994. Ship and satellite observations of chlorophyll stocks in interacting cyclone-anticyclone eddy pairs in the western Gulf of Mexico. Journal of Geophysical Research **99**:7371-7384.

Bretherton, F. P., Davis, R. E. & Fandry, C. B. A technique for objective analysis and design of oceanographic experiments applied to MODE-73. *Deep Sea Research* **23**, 559-582 (1976).

Brickman, D. and P.C. Smith. 2002. Lagrangian Stochastic Modeling in Coastal Oceanography. Journal of Oceanic and Atmospheric Technology, 19:83-99.

Brink, K. H. 1998. Wind-Driven Currents over the Continental Shelf. Pages 3-20 *in* K. H. Brink and A. R. Robinson, editors. The Sea. John Wiley & Sons.

Crone, T. J. and M. Tolstoy. 2010. Magnitude of the 2010 Gulf of Mexico Oil Leak. Science **330**:634-634.

Doyle, J. D., Q. Jiang, Y. Chao, and J. Farrara. 2009. High-resolution real-time modeling of the marine atmospheric boundary layer in support of the AOSN-II field campaign. Deep Sea Research Part II: Topical Studies in Oceanography **56**:87-99.

Fairall, C. W., E. F. Bradley, D. P. Rogers, J. B. Edson, and G. S. Young. 1996. Bulk parameterization of air-sea fluxes for TOGA COARE. Journal of Geophysical Research **101**:3747-3764.

Fingas, M. F. 1995. A Literature Review of the Physics and Predictive Modeling of Oil Spill Evaporation. Journal of Hazardous Materials **42**:157-175.

Fox, D. N., W. J. Teague, C. N. Barron, M. R. Carnes, and C. M. Lee. 2002. The Modular Ocean Data Assimilation System (MODAS). Journal of Atmospheric and Oceanic Technology **19**:240-252.

Hodur, R. M. 1997. The Naval Research Laboratory's Coupled Ocean/Atmosphere Mesoscale Prediction System (COAMPS). Monthly Weather Review **125**:1414-1430.

Hu, C., X. Li, W. G. Pichel, and F. E. Muller-Karger. 2009. Detection of natural oil slicks in the NW Gulf of Mexico using MODIS imagery. Geophysical Research Letters **36**:L01604.

Hu, C. 2010. Deepwater Horizon Disaster archive, MODIS RGB and SST images. University of South Florida, college of Marine Science, Optical Oceanography Laboratory. URL: http://optics.marine.usf.edu/events/GOM_rigfire/images/MODIS.2010131.184908.oil.rgb_oil_outline.png. Last Accessed 30 October 2013.

Hu, C., R. H. Weisberg, Y. Liu, L. Zheng, K. L. Daly, D. C. English, J. Zhao, and G. A. Vargo. 2011. Did the northeastern Gulf of Mexico become greener after the Deepwater Horizon oil spill? Geophysical Research Letters **38**:L09601.

Huntley, H. S., B. L. Lipphardt Jr., and A. D. Kirwan Jr. (2011), Surface drift predictions of the *Deepwater Horizon* spill: The Lagrangian perspective, in *Monitoring and Modeling the Deepwater Horizon Oil Spill: A Record-Breaking Enterprise*, Geophys. Monogr. Ser., vol. 195, edited by Y. Liu et al., pp. 179–195, AGU, Washington, D. C., doi:10.1029/2011GM001097.

Jolliff, J. K., J. C. Kindle, B. Penta, R. Helber, Z. Lee, I. Shulman, R. Arnone, and C. D. Rowley. 2008. On the relationship between satellite-estimated bio-optical and thermal properties in the Gulf of Mexico. Journal of Geophysical Research, Biogeosciences **113**:G01024, doi: 10.1029/2006JG000373.

Joye, S. B., I. R. MacDonald, I. Leifer, and V. Asper. 2011. Magnitude and oxidation potential of hydrocarbon gases released from the BP oil well blowout. Nature Geosci **4**:160-164.

Judson, R.S., M.T. Martin, D.M. Reif, K.A. Houck, T.B. Knudsen, D.M. Rotroff, M. Xia, S. Sakamuru, R. Huang, P. Shinn, C.P. Austin, R. J. Kavlock, D.J. Dix. 2010.

Analysis of Eight Oil Spill Dispersants Using Rapid, In Vitro Tests for Endocrine and Other Biological Activity. Environmental Science and Technology 44(15): 5979-5985. doi:10.1021/es102150z.

Kara, A. B., C. N. Barron, P. J. Martin, L. F. Smedstad, and R. C. Rhodes. 2006. Validation of interannual simulations from the $1/8^{o}$ global Navy Coastal Ocean Model (NCOM). Ocean Modelling **11**:376-398.

Ko, D. S., R. H. Preller, and P. J. Martin. 2003. An Experimental Real-Time Intra-Amercas Sea Nowcast/Forecast System for Coastal Prediction. Pages 97-100 *in* AMS 5th Conference on Coastal Atmospheric and Oceanic Prediciton and Processes.

Leben, R. R. and G. H. Born. 1993. Tracking Loop Current Eddies with satellite altimetry. Adv. Space Research **13**:325-333.

Ledwell, J.R., A.J. Watson, C.S. Law. 1998. Mixing of a tracer in the pycnocline. Journal of Geophysical Research, 103 (C10): 21,499-21,529.

Le Henaff, M., V.H. Kourafalou, C.B. Paris, J. Helgers, Z.M. Aman, P.J. Hogan, A. Srinivasan. 2012. Environmental Science and Technology 46(13):7267-7273. doi:10.1021/es301570w.

Leifer, I. 2010. Appendix 6: Riser Pipe Flow Estaimets, pp. 66 – 106. In: Deepwater Horizon Release Estimate of Rate by PIV. Plume Calculation Team. Report to Dr. Marcia McNutt, US Dept Interior. 215 pp.

Leifer, I., B. Luyendyk, and K. Broderick. 2006. Tracking an oil slick from multiple natural souces, Coal Oil Point, California. Marine and Petroleum Geology **23**:621-630.

Levy, J. K. and C. Gopalakrishnan. 2010. Promoting Ecological Sustainability and Community Resilience in the US Gulf Coast after the 2010 Deepwater Horizon Oil Spill. Journal of Natural Resources Policy Research **2**:297-315.

Liu, Y., R.H. Weisberg, C. Hu, and L. Zheng, 2011a. Trajectory Forecast as a Rapid Response to the Deepwater Horizon Oil Spill, in Monitoring and Modeling the Deepwater Horizon Oil Spill: A Record-Breaking Enterprise, Geophys. Monogr. Ser., vol. 195, edited by Y. Liu et al., pp. 91–101, AGU, Washington, D. C., doi:10.1029/2011GM001127.

Liu, Y., R. H. Weisberg, C. Hu, C. Kovach, and R. Riethmüller. 2011b. Evolution of the Loop Current system during the *Deepwater Horizon* oil spill event as observed with drifters and satellites, in Monitoring and Modeling the Deepwater Horizon Oil Spill: A Record-Breaking Enterprise, Geophys. Monogr. Ser., vol. 195, edited by Y. Liu et al., pp. 91–101, AGU, Washington, D. C., doi:10.1029/2011GM001127.

Lonin, S.A. 1999. Lagrangian Model for Oil Spill Diffusion at Sea. Spill Science & Technology Bulletin, 5(5/6): 331-336.

Maltrud, M., S. Peacock, M. Visbeck. 2010. On the possible long-term fate of oil released in the Deepwater Horizon incident, estimated using ensembles of dye release simulations. Environ. Res. Lett. 5, 035301.

Mariano, A.J., V.H. Kourafalou, A. Srinivasan, H. Kang, G.R. Halliwell, E.H. Ryan, and M. Roffer. 2011. On the modeling of the 2010 Gulf of Mexico Oil Spill. Dynamics of Atmospheres and Oceans, 52, 322-340.

Martin, P. J. 2000. Description of the Navy Coastal Ocean Model 1.0. NRL Report NRL/FR/7322/00/9962, 45 pp.

McNutt, M., R. Camilli, G. Guthrie, P. Hsieh, V. Labson, B. Lehr, D. Maclay, A. Ratzell, and M. Sogge. 2011. Assessment of Flow Rate Estimates for the Deepwater Horizon / Macondo Well Oil Spill. Flow Rate Technical Group Report to the National Incident Command, Interagency Solutions Group, March 10, 2011. U.S. Department of the Interior.

Michel, J., E. H. Owens, S. Zengel, A. Graham, A. Graham, Z. Nixon, T. Allard, W. Holton, P.D. Reimer, A. Lamarche, M. White, N. Rutherford, C. Childs, G. Mauseth, G. Challenger, and E. Taylor. 2013. Extent and Degree of Shoreline Oiling: *Deepwater Horizon* Oil Spill, Gulf of Mexico, USA. PLoS ONE 8(6): e65087. doi:10.1371/journal.pone.0065087

National Research Council, 2003. Oil in the Sea III: Inputs, Fates, and Effects. The National Academies Press. ISBN 0-309-08438-5. URL: http://books.nap.edu/catalog/10388.html.

Nelson, R. 2010. "New Computer tracking forecast shows oil reaching Florida Keys in five days, Miami in 10." U. S. Senate Press Release. Office of Senator Bill

Nelson, D-FL, Washington, D.C. URL: http://www.billnelson.senate.gov/news/details.cfm?id=326053&, Accessed 7 June 2013.

NOAA/NESDIS, 2013. National Environmental Satellite Information Service, Experimental Marine Pollution Surveillance Daily Composite Product. Digital Archive. ftp://satepsanone.nesdis.noaa.gov/OMS/disasters/DeepwaterHorizon/composites/2010/ Last accessed 30 October 2013.

NOAA OR&R. 2012. Open Water Oil Identification Job Aid for Aerial Observation with Standardized Oil Slick Appearance and Structure Nomenclature and Codes, Version 2. U.S. Department of Commerce, National Oceanic and Atmopsheric Administration, Office of Response and Restoration, Emergency Response Division, Seattle, Washington.

NOAA OR&R, 2013a. Deepwater Horizon Trajectory Map Archive. Web Document http://archive.orr.noaa.gov, last accessed 23 October 2013.

NOAA OR&R, 2013b. Environemntal Response Managament Application (ERMA) online mapping tool. http://gomex.erma.noaa.gov, last accessed 30 October 2013.

Obuko, A. 1971. Oceanic diffusion diagrams. Deep-Sea Research, Vol. 18: 789-802.

OSAT-2, Operational Science Advisory Team, Gulf Coast Incident Management Team. 2011. Summary Report for Fate and Effects of Remnant Oil in the Beach Environment. Prepared for Lincoln D. Stroh, CAPT, U.S. Coast Guard Federal On-Scene Coordinator Deepwater Horizon MC252. URL: http://www.restorethegulf.gov/sites/default/files/u316/OSAT-2%20Report%20no%20ltr.pdf

Paul J.H., D. Hollander, P. Coble, K.L. Daly, S. Murasko, D. English, J. Basso, J. Delaney, L. McDaniel, C.W. Kovach. 2013. Toxicity and mutagenicity of Gulf of Mexico waters during and after the Deepwater Horizon oil spill. Environmental Science & Technology 47(17):9651-9659. doi:10.1021/es401761h.

Proehl, J.A., D.R. Lynch, D.J. McGillicuddy Jr., and J. R. Ledwell. 2005. Modeling turbulent dispersion on the North Flank of Georges Bank using Lagrangian

Particle Methods. Continental Shelf Research, 25:875-900. doi:10.1016/j.csr.2004.09.022.

Rhodes, R. C., H. E. Hurlburt, A. J. Wallcraft, C. N. Barron, P. J. Martin, E. J. Metzger, J. F. Shriver, D.S. Ko, O. M. Smedstad, S. L. Cross, and A. B. Kara. 2002. Navy Real-time Global Modeling Systems. Oceanography **15**:29-43.

Rioux, P. 2010. "Oil washing ashore from Port Fourchon to Grand Isle", The Times-Picayune, Published 20 May 2010, 12:10 PM CDT. URL: http://www.nola.com/news/gulf-oil-spill/index.ssf/2010/05/tar_balls_wash_up_on_elmers_is.html. Last Accessed 13 June 2013.

Rosmond, T.E. 1992. The design and testing of the Navy Operational Global Atmospheric Prediction System. Weather Forecasting, 72(2): 262-272.

Rouse, L. J., Jr., W. J. Wiseman, and M. Inoue. 2005. Aspects of the Louisiana Coastal Current. U.S. Department of the Interior, Minerals Management Service, Gulf of Mexico OCS Region, New Orleans, LA. OCS Study MMS 2005-039. 50 pp.

Schmidt, K. 2010. "Oil hits Fourchon Beach," Houma Today. Published 15 May 2010, 0601 CDT. URL: http://www.houmatoday.com/article/20100515/ARTICLES/100519466.

Simpson, J. H. 1997. Physical processes in the ROFI regime. Journal of Marine Systems **12**:3-15.

Small, R. J., S. Carniel, T. Campbell, J. Teixeira, and R. Allard. 2012. The response of the Ligurian and Tyrrhenian Seas to a summer Mistral event: A coupled atmosphere–ocean approach. Ocean Modelling **48**:30-44.

Smolarkiewicz, P. K. 1984. A fully Multidimensional Positive Definite Advection Transport Algorithm with Small Implicit Diffusion. Journal of Computational Physics **54**:325-362.

Sobey, R.J. and C.H. Barker. 1997. Wave-driven transport of surface oil. Journal of Coastal Research 13(2):490-496.

Socolofsky, S. A., E. E. Adams, and C. R. Sherwood. 2011. Formation dynamics of subsurface hydrocarbon intrusions following the Deepwater Horizon blowout. Geophysical Research Letters **38**:L09602.

Sotillo, M. G., E. A. Fanjul, S. Castanedo, A. J. Abascal, J. Menendez, M. Emelianov, R. Olivella, E. García-Ladona, M. Ruiz-Villarreal, J. Conde, M. Gómez, P. Conde, A. D. Gutierrez, and R. Medina. 2008. Towards an operational system for oil-spill forecast over Spanish waters: Initial developments and implementation test. Marine Pollution Bulletin **56**:686-703

State of Louisiana, 2010. State of Louisiana Initial Oil Spill Respnse Plan, Deepwater Horizon Incident, 2 May 2010.

Sumaila, U. R., Andrés M. Cisneros-Montemayor, A. Dyck, L. Huang, W. Cheung, J. Jacquet, K. Kleisner, V. Lam, A. McCrea-Strub, W. Swartz, R. Watson, D. Zeller, and D. Pauly. 2012. Impact of the Deepwater Horizon well blowout on the economics of US Gulf fisheries. Canadian Journal of Fisheries and Aquatic Sciences **69**:499-510.

Tulloch, R., C. Hill, and O. Jahn. 2011. Possible Spreading of Buoyant Plumes and Local Coastline Sensitvities Using Flow Syntheses From 1992 to 2007, in Monitoring and Modeling the Deepwater Horizon Oil Spill: A Record-Breaking Enterprise Geophysical Monograph Series 195, Y. Liu, A. MacFadyen, Z.-G. Ji, R. H. Weisberg, Eds. (American Geophysical Union, Washington, D. C., 2011), vol. 195, pp. 245–255.

Walker, N., C. Pilley, E. D'Sa, R. Leben, P. Coholan, P. Brickley, and H. Graber. 2012. Loop Current eddy merger exposed by satellites during Gulf of Mexico oil spill. 13 September 2012, SPIE Newsroom. DOI: 10.1117/2.1201209.004439

Weisberg, R. H. and R. He. 2003. Local and deep-ocean forcing contributions to anomalous water properties on the West Florida Shelf. Journal of Geophysical Research **108**:3184. doi:10.1029/2002JC001407.

Wiseman, Jr., W. J. and S. P. Dinnel. 1988. Shelf currents near the mouth of the Mississippi River. Journal of Physical Oceanography **18**:1287-1291. doi: http://dx.doi.org/10.1175/1520-0485(1988)018<1287:SCNTMO>2.0.CO;2

Zelenke, B., C. O'Connor, C. Barker, C. J. Beegle-Krause, and L. Eclipse (Eds.). 2012. General NOAA Operational Modeling Environment (GNOME) Technical Documentation. U.S. Dept. of Commerce, NOAA Technical Memorandum NOS OR&R 40. Seattle, WA: Emergency Response Division, NOAA. 105 pp. URL: http://response.restoration.noaa.gov/sites/default/files/GNOME_Tech_Doc.pdf

Zengel, S. and J. Michel. 2013. Deepwater Horizon Oil Spill: salt marsh oiling conditions, treatment testing, and treatment history in northern Barataria Bay, Louisiana. Seattle: NOAA Technical Memorandum 42, Office of Response and Resoration. 74 pp.

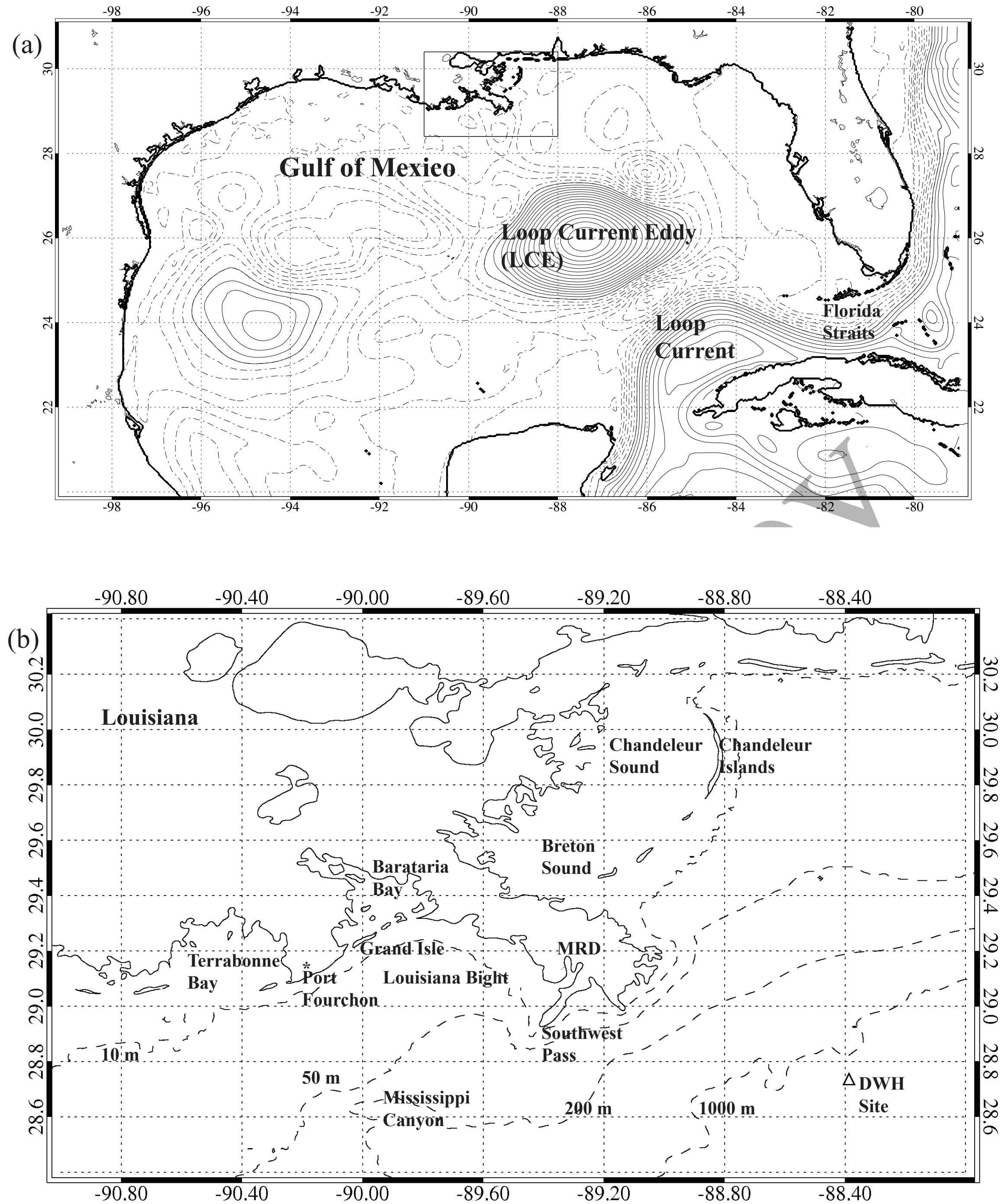

Figure 1. (a) Map of the Gulf of Mexico with Sea Surface Height (SSH) contours (positive solid, negative dashed) provided by the IASNFS (29 May 2010). The Loop Current (LC) and an associated Loop Current Eddy (LCE) are indicated. Inset and (b): detailed map of the Louisiana coastal region near the DWH site. Bathymetry is indicated with dashed lines.

(a)

(b)

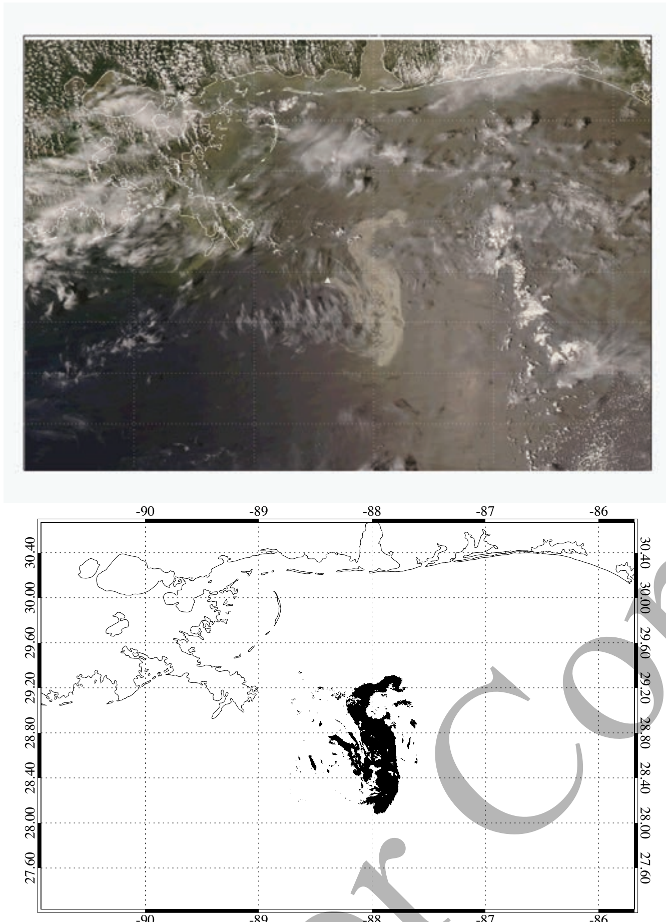

Figure 2. MODIS data acquired 11 May 2010, 18:55 UTC (250 m horizontal resolution) and processed as a true color image is shown in plate (a). In (b) the apparent position of the surface oil slicks are extracted from the image, as explained in the text.

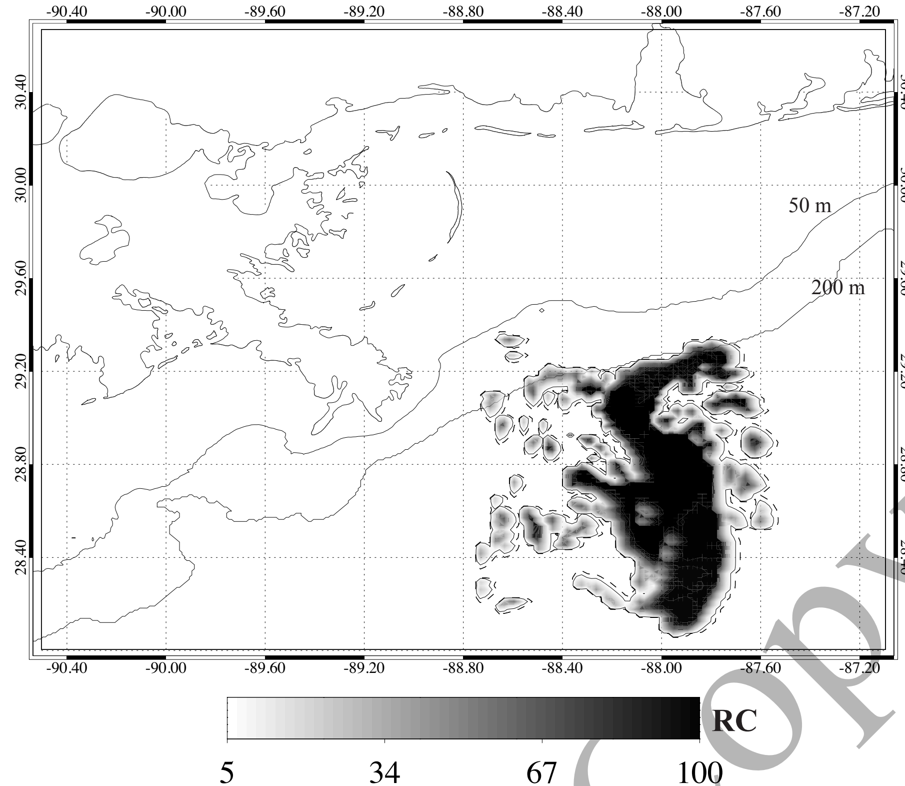

Figure 3. The initial estimate of surface oil slick distribution extracted from the MODIS image is mapped to the inner ocean model domain of COAMPS (500 m horizontal resolution) for the beginning of an oil trajectory forecast. The oil forecast output increment (+1 hour) is shown for 11 May 2010, 2000 UTC. RC is the Relative Concentration, scaled to the initial oil distribution estimate, RC = 100. The dashed line indicates RC = 1, the solid line begins the contours at RC = 5.

(a)

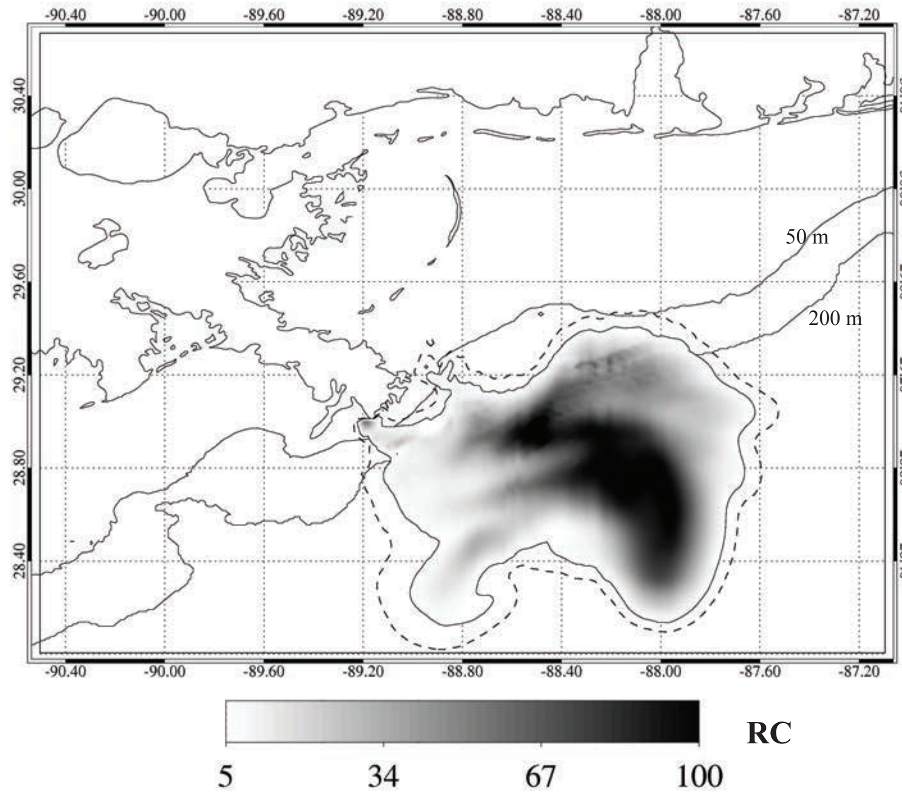

(b)

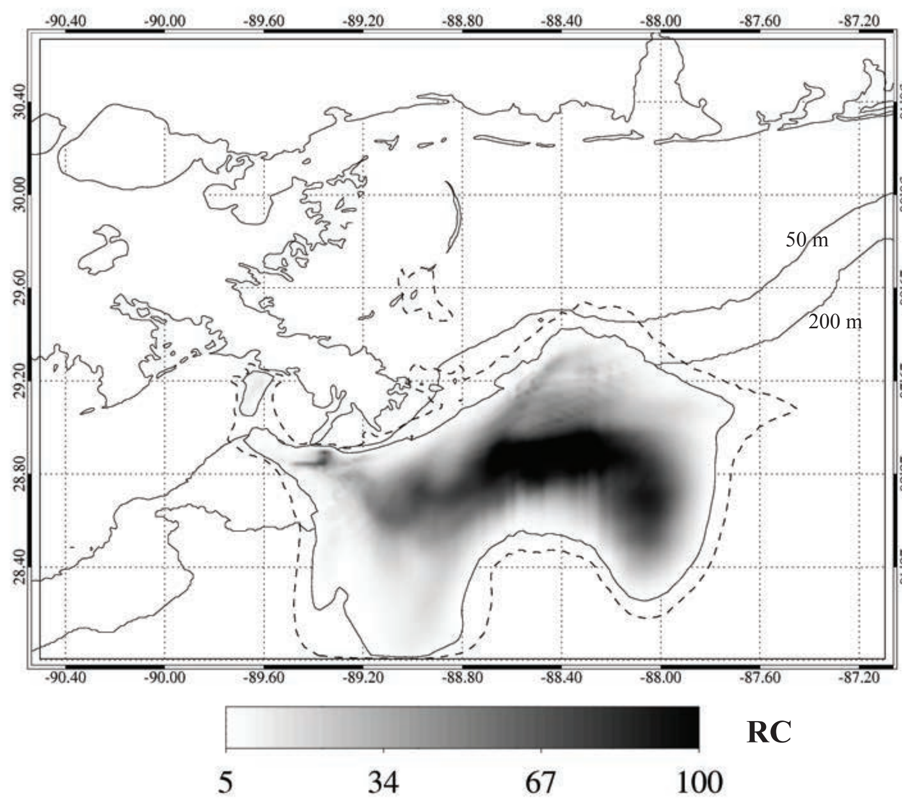

Figure 4. (a) Oil transport forecast for 12 May 2010, 1900 UTC, and (b) oil transport forecast for 13 May 2010, 1900 UTC. The dashed line indicates RC = 1, the solid line begins the contours at RC = 5.

(a)

(b)

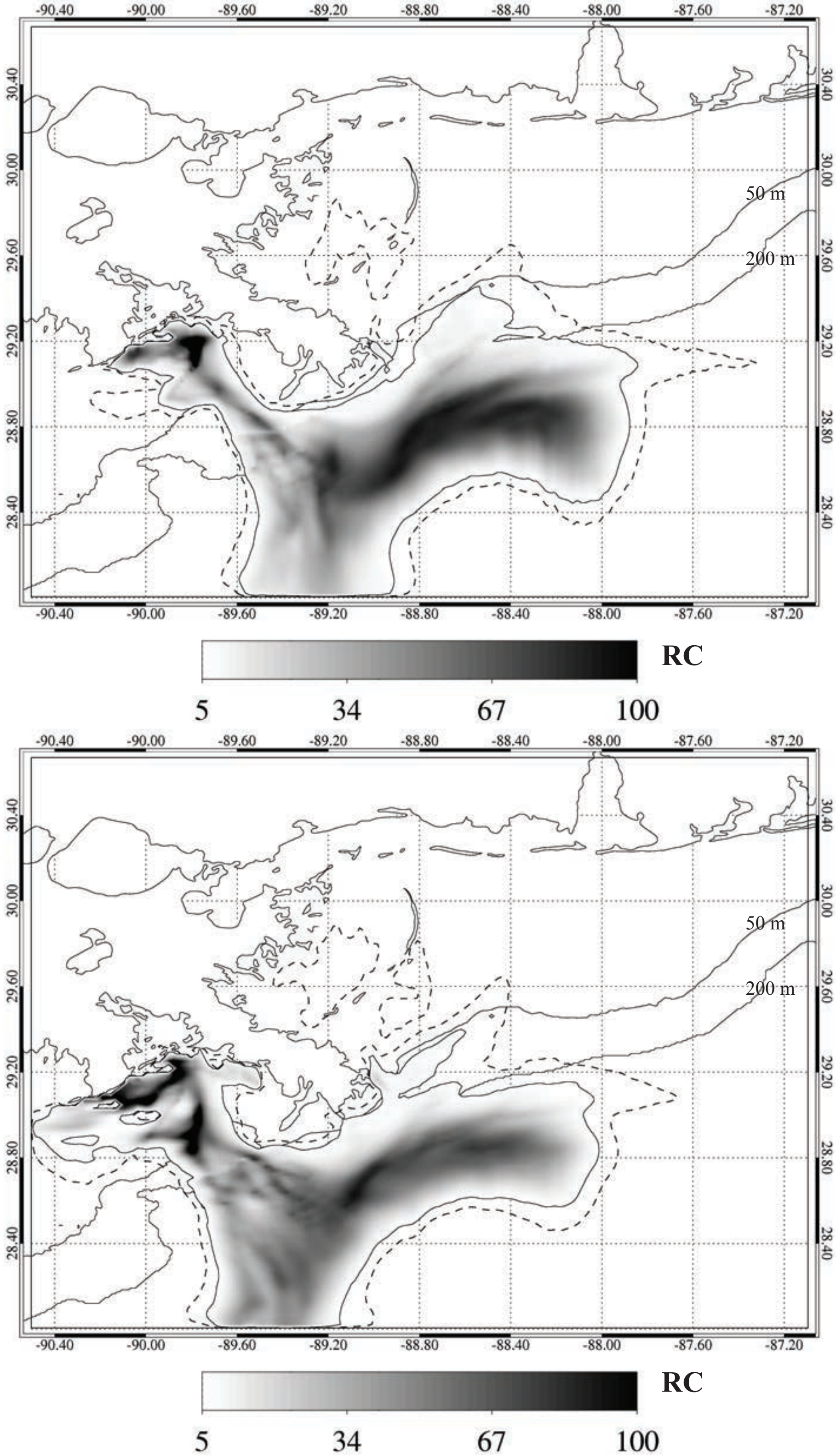

Figure 5. (a) Oil transport forecast for 14 May 2010, 2100 UTC, and (b) oil transport forecast for 15 May 2010, 1900 UTC. The dashed line indicates RC = 1, the solid line begins the contours at RC = 5.

(a)

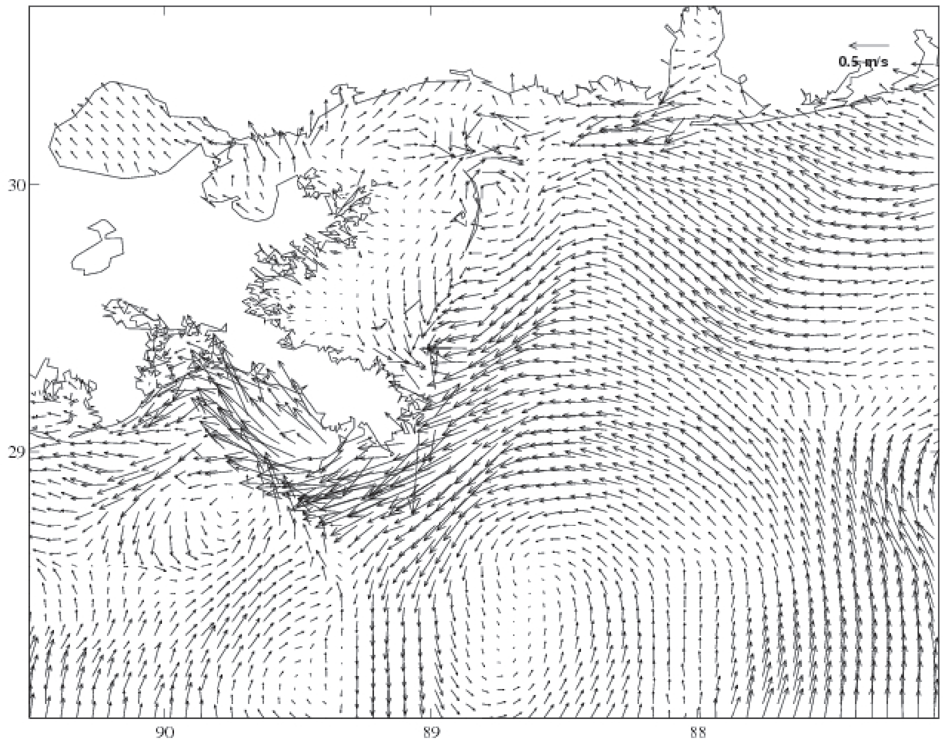

(b)

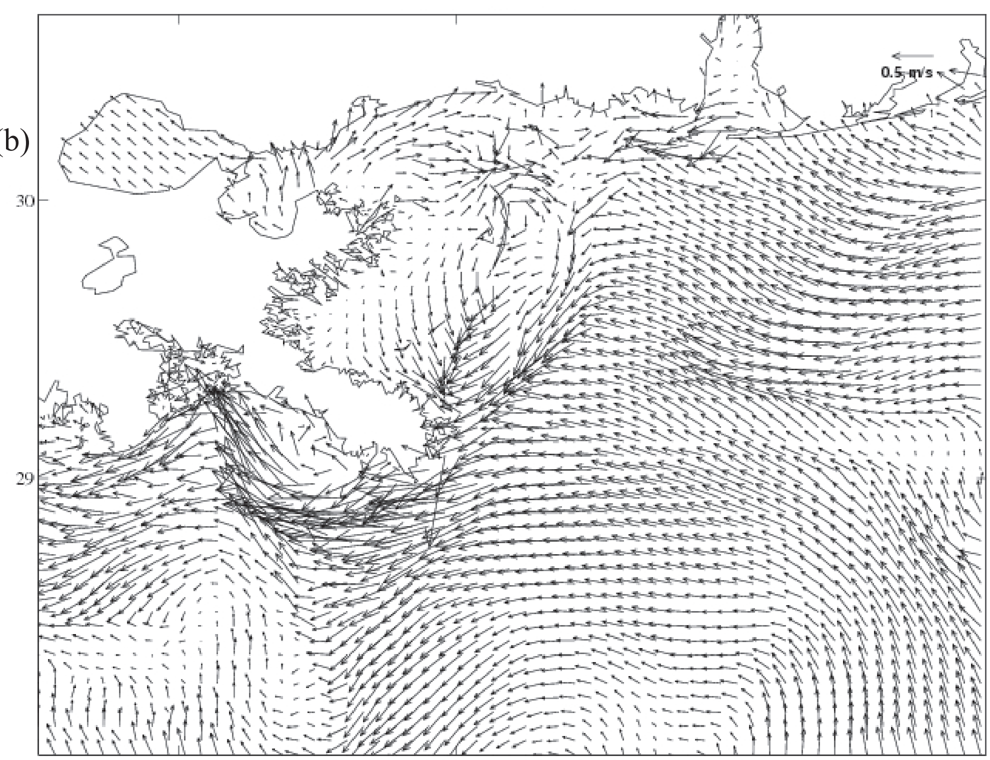

Figure 6. (a) COAMPS surface current velocity field forecast for 14 May 2010, 1700 UTC, and (b) COAMPS surface current velocity field forecast for 14 May 2010, 1700 UTC.

(a)

(b)

(c)

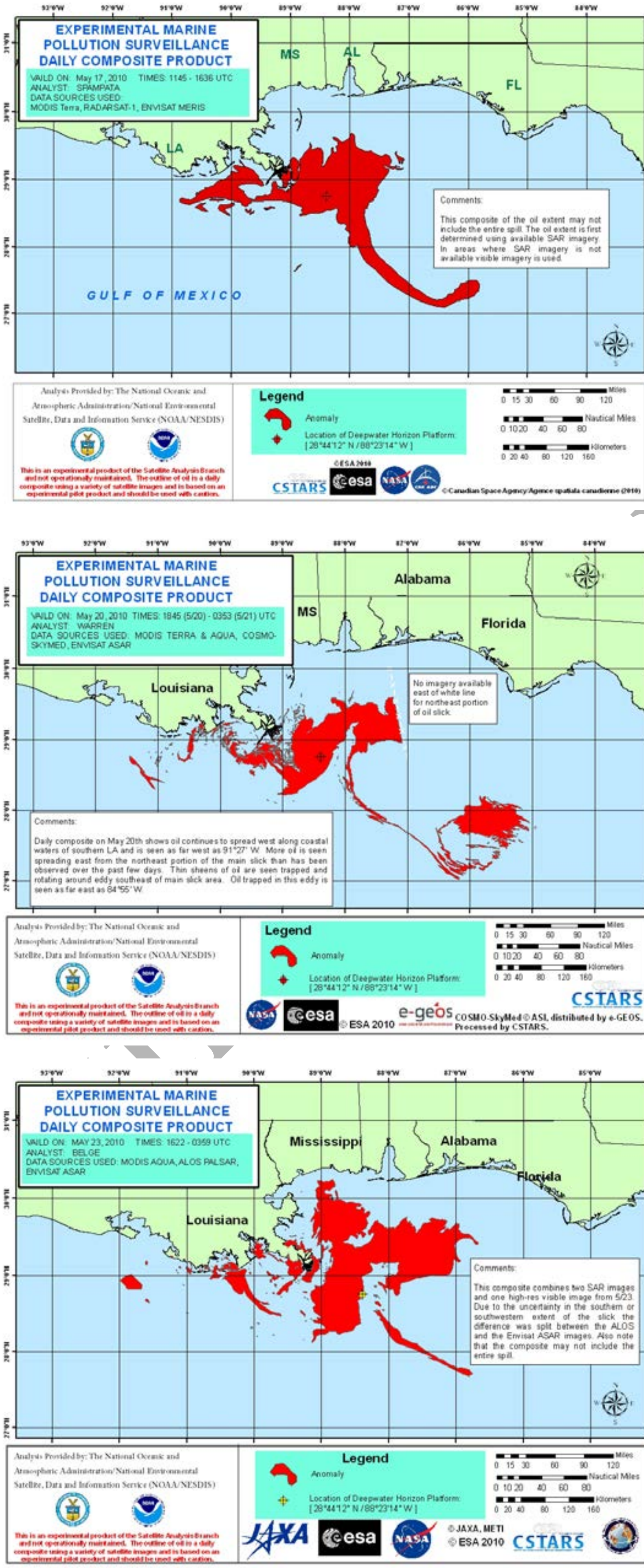

Figure 7. Composite satellite analysis of potential surface oil location obtained from the NOAA/NESDIS archive for (a) 17 May 2010, (b) 20 May 2010, and (c) 23 May 2010.

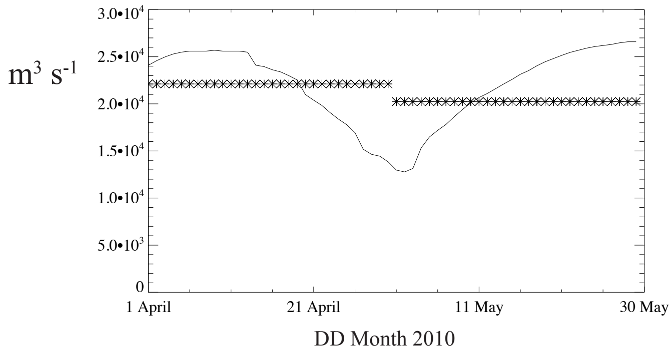

Figure 8. Discharge data (solid line) for Mississippi River at Tarbert Landing (United States Army Corps of Engineers) are shown in cubic meters per second. The asterisks (*) indicate the climatological monthly means used for the COAMPS simulations.

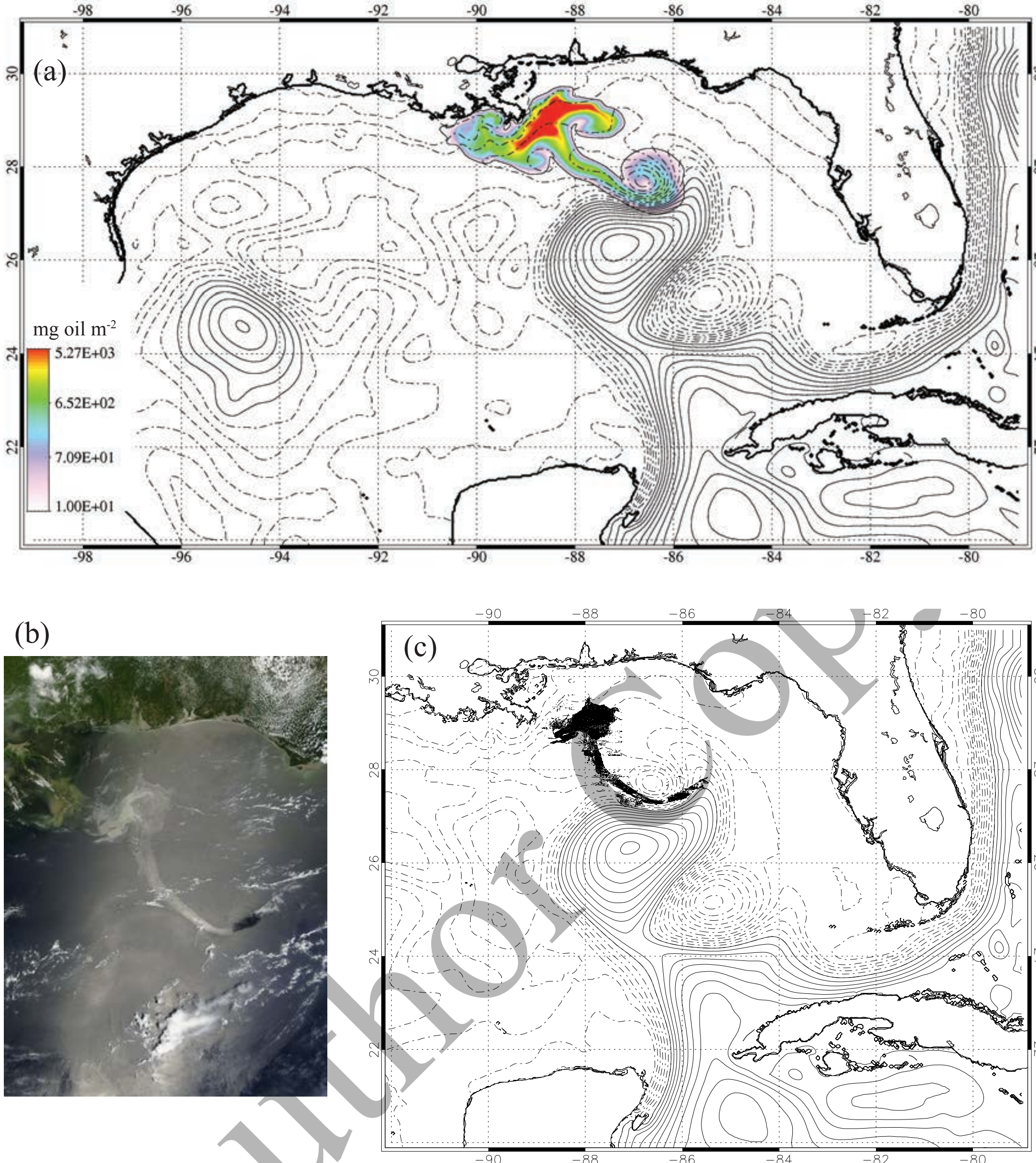

Figure 9. (a) Regional oil model result for 17 May 2010, 1800 UTC. SSH contours (positive solid, negative dashed) provided by the corresponding IASNFS fields. (b) MODIS true color image acquired on 17 May 2010, 1640 UTC. (c) The estimate of visible oil is mapped to the model domain and shown in black.

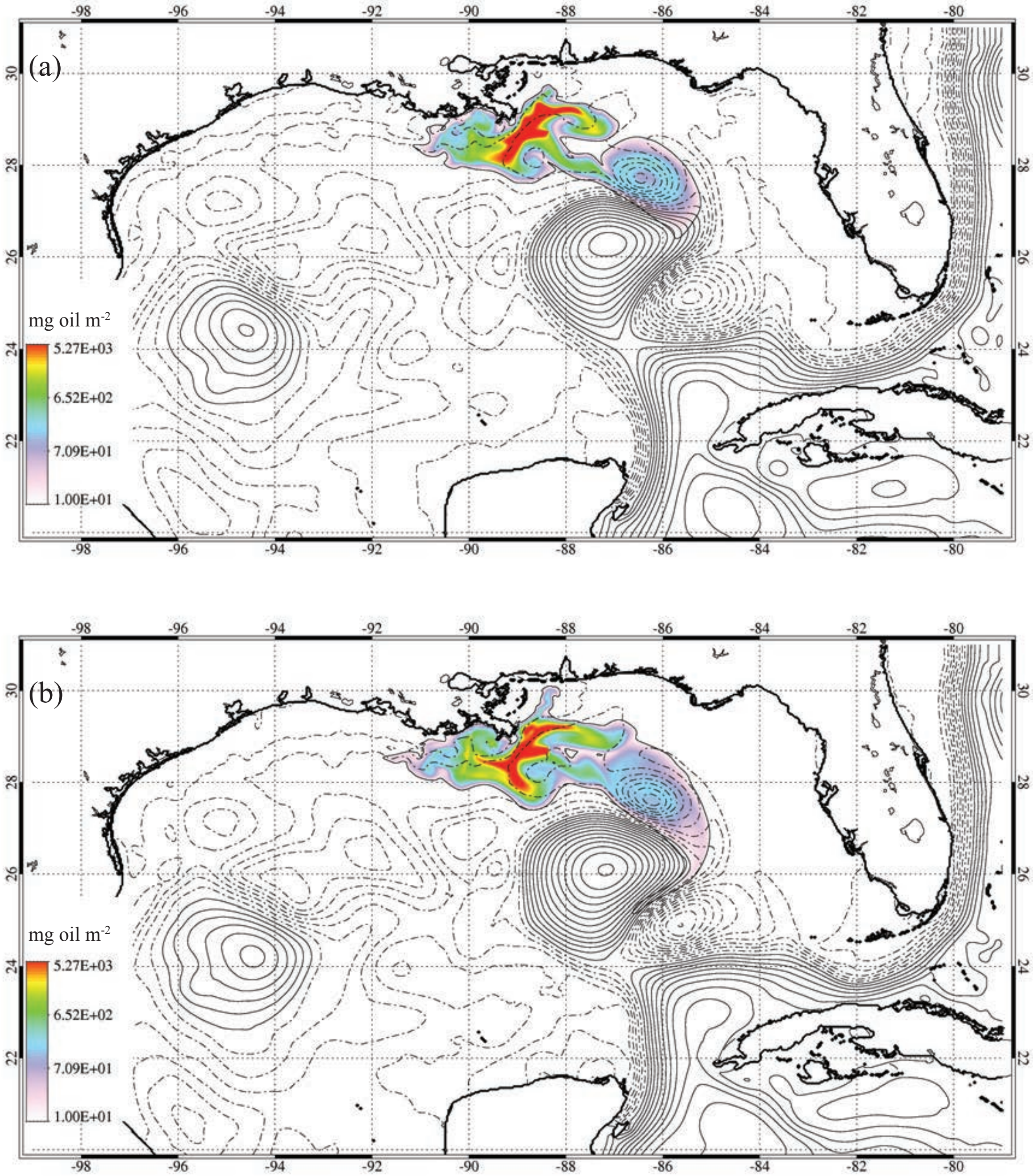

Figure 10. (a) Regional oil model result for 19 May 2010, 1200 UTC. (b) Regional oil model result for 22 May 2010, 0600 UTC.

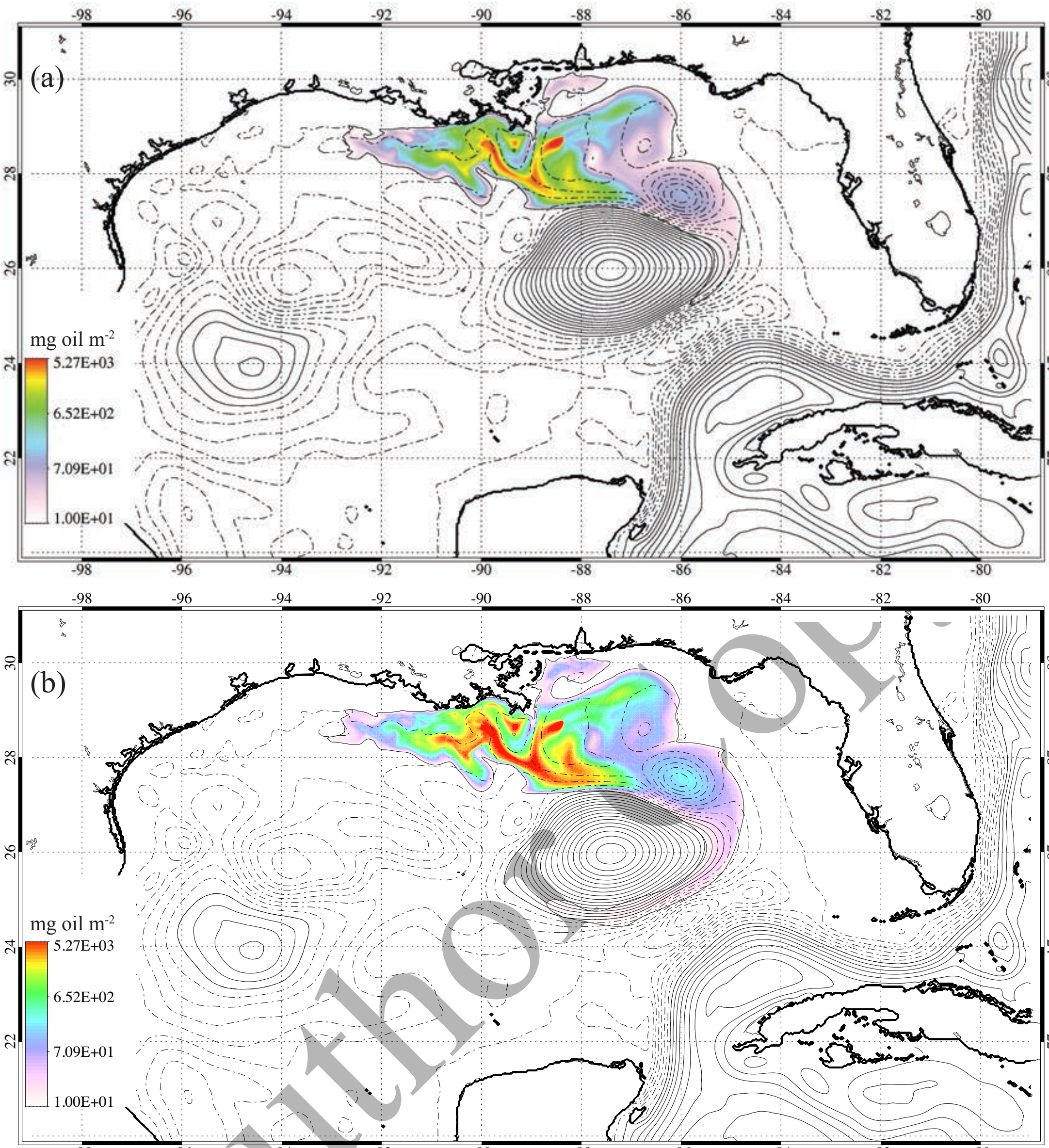

Figure 11. (a) Regional oil model result for 29 May 2010, 0600 UTC. (b) Regional oil model result for the NL simulation 29 May 2010, 0600 UTC.

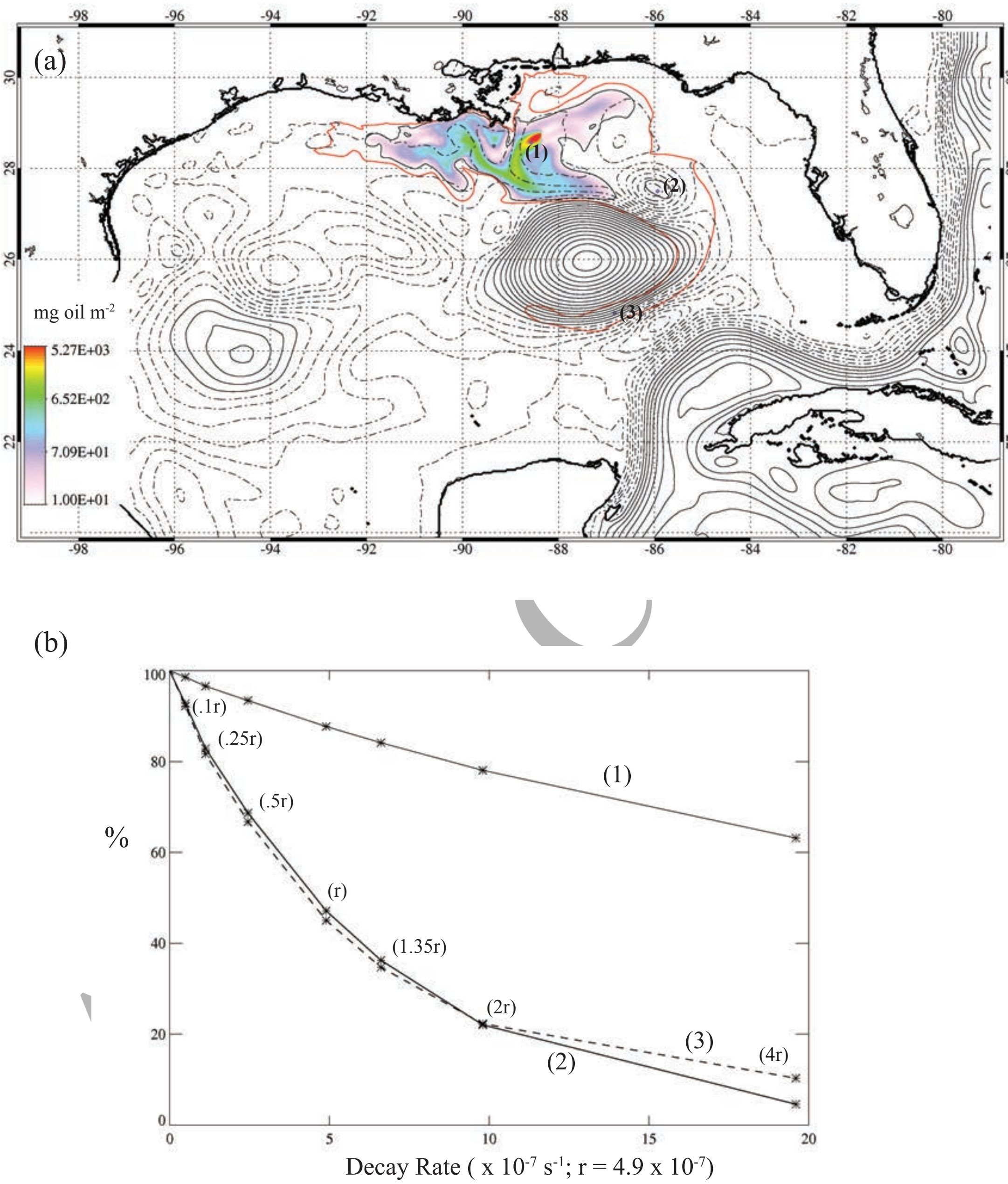

Figure 12. (a) Regional oil model result for 29 May 2010, 0600 UTC using the (4r) decay rate sensitivity simulation is contoured as in Figure 11. The contour of the NL simulation 10 mg oil m^{-2} surface isopleth is shown in red. (b) Sensitivity analysis for surface oil concentrations indicated in (a). The surface concentration values for each different simulation (varying values of r) is normalized by the corresponding value in the NL simulation and expressed as a percentage.